Molecular Biology of the Cell
Vol. 10, 4283–4298, December 1999

Nuclear Accumulation of *S*-Adenosylhomocysteine Hydrolase in Transcriptionally Active Cells during Development of *Xenopus laevis*

Norbert Radomski, Christine Kaufmann, and Christine Dreyer*

Max-Planck-Institut für Entwicklungsbiologie, D-72076 Tübingen, Germany

Submitted June 10, 1999; Accepted September 8, 1999
Monitoring Editor: Joseph Gall

The oocyte nuclear antigen of the monoclonal antibody 32-5B6 of *Xenopus laevis* is subject to regulated nuclear translocation during embryogenesis. It is distributed in the cytoplasm during oocyte maturation, where it remains during cleavage and blastula stages, before it gradually reaccumulates in the nuclei during gastrulation. We have now identified this antigen to be the enzyme *S*-adenosylhomocysteine hydrolase (SAHH). SAHH is the only enzyme that cleaves *S*-adenosylhomocysteine, a reaction product and an inhibitor of all *S*-adenosylmethionine-dependent methylation reactions. We have compared the spatial and temporal patterns of nuclear localization of SAHH and of nuclear methyltransferase activities during embryogenesis and in tissue culture cells. Nuclear localization of *Xenopus* SAHH did not temporally correlate with DNA methylation. However, we found that SAHH nuclear localization coincides with high rates of mRNA synthesis, a subpopulation colocalizes with RNA polymerase II, and inhibitors of SAHH reduce both methylation and synthesis of poly(A)$^+$ RNA. We therefore propose that accumulation of SAHH in the nucleus may be required for efficient cap methylation in transcriptionally active cells. Mutation analysis revealed that the C terminus and the N terminus are both required for efficient nuclear translocation in tissue culture cells, indicating that more than one interacting domain contributes to nuclear accumulation of *Xenopus* SAHH.

INTRODUCTION

Regulated localization of nuclear factors is an important mechanism for modulation of nuclear activities. Regulated translocation can be clearly observed during embryonic development, as cells successively undergo a sequence of different physiological states. In vertebrate embryogenesis, regulated nuclear translocation of maternal nuclear proteins was first detected in *Xenopus laevis* (Dreyer *et al.*, 1982, 1985; Dreyer and Hausen, 1983; Dreyer, 1987). In early development of *X. laevis*, growth and cell division are uncoupled. A pool of maternal mRNA and protein accumulates during the several months of oocyte growth, and this pool enables the fertilized egg to undergo a rapid sequence of cleavage divisions. As shown with application of mAbs raised against oocyte nuclear proteins, maternal nuclear proteins are shed into the cytoplasm during oocyte maturation and reassembled in the nuclei of the embryo. Plausibly, proteins engaged in replication, chromatin assembly, and nuclear architecture, such as nucleoplasmin, N1, N2, and lamin B3, accumulate in cleavage nuclei, whereas some others, including nucleolin (Messmer and Dreyer, 1993; Schwab and Dreyer, 1997) and xNF7, a zinc finger protein of the ret proto-oncogene family (Miller *et al.*, 1991), remain predominantly cytoplasmic until blastula stages (for review, see Dreyer, 1989). In several instances, nuclear translocation of a protein is restricted to a specific cell lineage or region of the embryo at a given time; e.g., regulated nuclear translocation of myoD is observed in the dorsal mesoderm (Rupp *et al.*, 1994), and a fraction of β-catenin becomes nuclear first in the dorsal and later in the ventral lateral zone of the *Xenopus* embryo (Schneider *et al.*, 1996), potentially as a part, or consequence, of the activated wnt signal transduction cascade (Crease *et al.*, 1998). SMADs, a class of transcription factors involved in dorsoventral patterning in *X. laevis*, translocate to the nucleus in response to members of the transforming growth factor β–activin–bone morphogenic protein family in a ligand-specific manner (Heldin *et al.*, 1997; Liu *et al.*, 1997; Suzuki *et al.*, 1997; Nomura and Li, 1998).

* Corresponding author. E-mail addresss: Christine.Dreyer@tuebingen.mpg.de.

Abbreviations used: aa, amino acid; BrdU, bromodeoxyuridine; DMA, 2′-deoxy-1-methyladenosine; DRB, 5,6-dichloro-1-β-D-ribofuranosylbenzimidazole; GCG, Genetics Computer Group; hnRNA, heterogenous nuclear RNA; IIF, indirect immunofluorescent; MBT, midblastula transition; MT, myc-tagged; PB, physiological buffer; SAHH, *S*-adenosylhomocysteine hydrolase; SAM, *S*-adenosylmethionine; xSAHH, *Xenopus* SAHH.

Among the previously unidentified maternal nuclear antigens that are subject to stage-specific nuclear translocation in *Xenopus* embryos is the enzyme *S*-adenosylhomocysteine hydrolase (SAHH; EC 3.3.1.1). This enzyme cleaves a byproduct of all *S*-adenosylmethionine (SAM)-dependent methylation reactions, S-adenosylhomocysteine, which would interfere with methylation by product inhibition. The fact that inhibition of SAHH by nucleoside homologues efficiently inhibits methyltransferases (Ueland, 1982; Kramer *et al.*, 1990) shows the importance of this enzyme for biological transmethylation reactions. Although SAM-dependent methylation reactions occur in different compartments of the cell, SAHH has previously been described as a cytoplasmic enzyme (Hershfield and Krodich, 1978; Turner *et al.*, 1997). Although the low-molecular-weight substrate *S*-adenosylhomocysteine should be able to diffuse to the cytoplasm after production in the nucleus, the efficiency of transmethylation might profit from a close proximity between the methyltransferase and SAHH. To get some insight into the physiological significance of the nuclear localization of *Xenopus* SAHH (xSAHH), we have correlated it to nuclear methylation reactions. To identify the structural requirements for nuclear accumulation of xSAHH, we have investigated the localization of deletion mutants expressed in tissue culture cells.

MATERIALS AND METHODS

Isolation of cDNAs

An *X. laevis* ovary cDNA library unidirectionally cloned in the Uni-ZAP XR vector (Stratagene, Heidelberg, Germany) was screened with application of mAb 32-5B6 for phage plaques expressing the antigen, essentially as described previously (Messmer and Dreyer, 1993). Of $\sim 5 \times 10^5$ phages seeded, 6 expressed polypeptides that reacted with the mAb, and 5 of these were successfully plaque purified. In vivo excision of the cDNA in pBluescript SK(−) using the exassist helper phage/SOLR system was performed according to the manufacturer's protocol (Stratagene). Sequencing of the cDNAs was performed with an A.L.F. Sequencer (Pharmacia Biotech, Freiburg, Germany) using vector-specific and gene-specific primers synthesized by MWG-Biotech (Ebersberg, Germany). Sequence analysis was performed using the Genetics Computer Group (GCG; Madison, WI) software package (Wisconsin Package version 9.1).

For transfection experiments, an *Eco*RI–*Xho*I fragment of the xSAHH2 cDNA, containing the complete open reading frame was subcloned into the pCS2+MT vector (Rupp *et al.*, 1994; Turner and Weintraub, 1994) for expression of the myc-tagged (MT)-xSAHH fusion protein. The 1373-bp *Rca*I (refilled)–*Cla*I fragment of pCS2+MT-xSAHH was subcloned into *Xho*I (refilled)–*Cla*I-digested pCS2+MT to construct pCS2+MT-xSAHHΔ361–433. For expression of MT-xSAHHΔ425–433, pCS2+MT-xSAHH was digested with *Dra*II–*Xho*I, refilled, and religated. Frame shift mutations were induced in pCS2+MT-xSAHH with application of the Quick Change site-directed mutagenesis kit (Stratagene). In brief, pCS2+MT-xSAHHΔ1–13 and Δ1–21 were generated by removing a single base pair from the linker region and inserting a base pair in the 13th or 21st codon of the SAHH sequence, respectively, as shown in Figure 8B. pCS2+MT-xSAHHΔ402–433 was produced by inserting one base into the codon of aa 401, resulting in substitution of aa 402–424, followed by a stop codon.

Protein Microsequencing

Protein extracts were prepared from oocytes as described previously (Dreyer *et al.*, 1982), diluted threefold with 20 mM triethanolamine, pH 8.0, and loaded on a 10-ml Source Q anion exchange column (Pharmacia Biotech). After elution with a linear salt gradient (0–0.5 M NaCl in 20 mM triethanolamine), fractions containing the antigen of mAb 32-5B6 were identified by Western blotting. Peak fractions of material eluted with ~0.1 M NaCl were precipitated with acetone and separated on two-dimensional gels as described previously (Dreyer and Hausen, 1983). After 10 min of capillary blotting onto a sheet of nitrocellulose, the position of the antigen was identified, and the antigen-containing area was excised from the gel and stored at −70°C. Antigenic material of 14 two-dimensional gels was pooled. Stained gel fragments were washed three times with water and three times with 50% acetonitrile and 50% 0.1 M ammonium bicarbonate. The washed gel fragments were incubated with 1 μg of trypsin (Promega, Madison, WI) in 300 μl of 0.1 M ammonium bicarbonate for 16 h at 37°C. The supernatant was removed, and the gel fragments were extracted at 57°C for 45 min with 50% trifluoroacetic acid and 50, 50, and 80% acetonitrile. The pooled supernatants were concentrated nearly to dryness using a SpeedVac apparatus (Savant Instruments, Holbrook, NY). Peptides were separated on a Vydac (Hesperia, CA) 218 TP51 column with a linear gradient between 0.1% trifluoroacetic acid and 70% acetonitrile. An Applied Biosystems (Foster City, CA) sequenator (model A470) and a Knauer (Berlin, Germany) sequenator (model 810), both equipped with on-line phenylisothiocyanate amino acid analyzers, were used for automated sequencing. For one of the tryptic peptides expected from the cDNA-deduced sequence (aa 170–187), only residues 175–187 were unambiguously identified.

Genomic DNA Preparation

Embryos of *X. laevis* were staged according to the method of Niewkoop and Faber (1967). DNA from desired stages was extracted as described (Sambrook *et al.*, 1989). Briefly, embryos were powdered in liquid nitrogen and incubated in extraction buffer (10 mM Tris-HCl, pH 8.0, 100 mM EDTA, 0.5% SDS, 20 μg/ml RNase) for 1 h at 37°C, followed by proteinase K digestion (100 μg/ml) for 12 h at 55°C. The DNA was purified by five cycles of organic solvent extraction and precipitated with ethanol.

Assay of 5-Methylcytosine in CpG-containing Sequences

Total DNA was isolated from embryos of different stages, and the degree of methylation in CpG-containing sequences was determined by a modified nearest-neighbor analysis (Gruenbaum *et al.*, 1981). Five to 10 μg of DNA were nicked with 10 U of DNase I (Boehringer Mannheim, Mannheim, Germany) for 15 min at 37°C and 3′-end labeled with 25 μCi of [α^{32}P]dGTP (3000 Ci/mmol; Amersham, Braunschweig, Germany) and 10 U DNA polymerase I (Sigma, Deisenhofen, Germany) for 30 min at 15°C in a 25-μl reaction mixture containing 50 mM Tris-HCl, pH 7.5, 5.0 mM $CaCl_2$, and 0.04% β-mercaptoethanol. After termination by 10 mM EDTA, nonincorporated dGTP was removed using a Sephadex G-50 minicolumn (Boehringer Mannheim). Labeled DNA was precipitated with ethanol, dissolved in 25 mM Tris-HCl, pH 8.0, and 5.0 mM $CaCl_2$, and digested with 2 U of micrococcal nuclease (Sigma) followed by treatment with 2 U of spleen phosphodiesterase II (Sigma) for 1 h at 37°C each. The resulting desoxynucleoside 3′-monophosphates were applied to cellulose TLC sheets (Machery-Nagel, Düren, Germany) and separated in two dimensions (Gruenbaum *et al.*, 1981). Chromatograms were analyzed using phosphor screens, a Storm 820 scanner, and the ImageQuant 1.2 software package (Molecular Dynamics, Sunnyvale, CA). The percentage of methylated CpG was determined after quantification of m^5C and C.

Cell Culture

A6 (*Xenopus* kidney epithelium cells, CCL 102; American Type Culture Collection, Manassas, VA) and XTC (*Xenopus* tadpole cells;

Pudney *et al.*, 1973) cell lines were grown in RPMI 1640 medium (Life Technologies, Eggenstein, Germany) supplemented with 15% H_2O, 10% FCS (Biochrom KG Seromed, Berlin, Germany), 100 IU/ml penicillin, and 100 μg/ml streptomycin (Life Technologies) at 25°C in a 5% CO_2 atmosphere. For LipofectAMINE transfection experiments (Life Technologies) cells were adapted to Dulbecco's modified Eagle's medium supplemented as described above.

Cell Cycle Analysis

XTC cells were arrested in G0 by cultivation in medium containing 0.5% FCS for 3 d. Subsequently, the cultures were washed with PBS containing 15% H_2O, and medium containing 10% FCS was added. After serum stimulation, samples were taken at intervals as indicated, washed, fixed with ice-cold ethanol containing 5% acetic acid, and processed for indirect immunofluorescence staining. Progression into S phase was monitored by incorporation of bromodeoxyuridine (BrdU; 10 μM final concentration) for 1 h before fixation and subsequent immunofluorescence staining with an anti BrdU mAb (Boehringer Mannheim; see below). The ethanol/acetic acid fixation allowed optimal detection of the BrdU-labeled DNA but was suboptimal for detection of xSAHH by mAb 32-5B6.

Transient Transfection

Twenty-four hours before transfection, 2×10^4 A6 cells were seeded on glass coverslips (1 cm in diameter) in a 24-well tissue culture plate. Subsequently, the medium was replaced by serum-free medium (Optimem, Life Technologies) before transfection with 1 μg of plasmid and 3 μl of lipid transfection agents (LipofectAMINE) per well and 750 μl of serum-free medium. After 3–12 h cultures were washed, incubated in medium containing 10% FCS for 24–120 h, fixed with 3.7% formaldehyde, and processed for indirect immunofluorescence (mAb 9E10).

Br-UTP Incorporation in Permeabilized Cells (Run-on Transcription)

Cells on Coverslips. Frog cells lines grown to subconfluent density were first washed in ice-cold PBS supplemented with 15% H_2O and then with physiological buffer (PB; Jackson *et al.*, 1993), adapted to frog cells by addition of 15% H_2O (final concentration, 9.6 mM Na_2HPO_4, pH 7.4, 87 mM sodium acetate, 26 mM KCl, 0.87 mM $MgCl_2$, 1.0 mM dithiothreitol, 0.2 mM phenylmethylsulfonylfluride, and 20 U/ml RNase inhibitor). Cells were permeabilized in PB containing 40 μg/ml digitonin for 5 min on ice and washed with PB, and nascent RNA was labeled for 5–10 min at 25°C with PB including 0.5 mM ATP, CTP, GTP, Br-UTP, and 2 mM $MgCl_2$. In some experiments, α-amanitin (10 μg/ml) or 2′-deoxy-1-methyladenosine (DMA; 1 or 5 mM) was present. Labeled cells were successively washed with PB and 0.5% Triton X-100 in PB, 3 min each, fixed with 3.7% formaldehyde in PB for 10 min. Fixed cells were washed with PB and processed immediately for indirect immunofluorescence or stored in absolute ethanol at −20°C.

Embryos. Embryos of desired stages were injected with 50 nl of PB containing 1.5 mM ATP, CTP, GTP, and Br-UTP and 120 μg/ml digitonin with or without 50 μg/ml α-amanitin and incubated 30–60 min at 23°C. Then embryos were fixed with 3.7% formaldehyde in PB for 2 h at room temperature, divided in halves along the animal to vegetal axis, additionally fixed at 4°C for 12 h, and processed immediately for indirect immunofluorescence or stored in absolute ethanol at −20°C.

Indirect Immunofluorescent (IIF) Staining

Cells grown on glass coverslips were fixed (if not otherwise stated) with 3.7% formaldehyde in PBS for 10 min and permeabilized for 5 min with 0.5% Triton X-100 and 3.7% formaldehyde in PBS. Blocking was performed with 20% bovine serum in IIF dilution buffer (PBS containing 2% bovine serum, 2.5% cold water fish gelatin, 10% glycerol, 0.1% Tween 20, and 2% normal serum corresponding to the selected secondary antibody) for 15 min. Incubations with primary and secondary antibodies were for 45 min each, followed by several washes in PBS containing 0.1% Tween 20. Cells were additionally fixed, counterstained with DAPI (0.5 μg/ml) to identify cell nuclei and mitotic chromosomes, and mounted in elvanol (15% Mowiol 4–88 [Hoechst, Frankfurt, Germany], 30% glycerol in PBS) containing 10% 1,4-diazabicyclo[2.2.2]octane. For staining of cells after run-on transcription all solutions were supplemented with RNase inhibitor (40 U/ml; Stratagene). Antibodies were as follows: mAb 32-5B6 (1:200) or mouse anti-myc tag (1:1000; clone 9E10) followed by goat anti-mouse Cy3 (1:500; Dianova, Hamburg, Germany); mAb 32-5B6 (1:200) plus rat-anti-BrdU (1:20; Sera-Lab, Crawley Down, United Kingdom) followed by donkey anti-mouse Cy3-$(Fab)_2$ (1:200; Dianova) and donkey anti-rat Cy2-$(Fab)_2$ (1:50; Dianova); and mAb anti-BrdU (1:10; Boehringer Mannheim) followed by goat anti-mouse 5-([4,6-dichlorotriazin-2-yl]amino)-fluorescein (1:50; Dianova).

For staining of embryo halves, the time for the incubation steps was increased as follows: blocking, 30 min; washing steps, four times for 30 min each; antibody incubation, 3 h at room temperature or 10 h at 4°C; and postantibody fixation, 30 min. Note that only the superficial cell layer was stained by this procedure.

Whole-mount staining and sectioning of complete embryos were performed as described (Ellinger-Ziegelbauer and Dreyer, 1993) with minor modifications. Incubation times were increased to at least 40 h at room temperature for the first antibody and to 24 h at room temperature for the secondary antibody, and 2.5% DMSO was added to the IIF dilution buffer.

Frozen sections were prepared from ovaries of young females prefixed with 4% paraformaldehyde for 3 h and Dent's fixative overnight at −20°C as described (Fagotto and Gumbiner, 1994). The mAb H14 (immunoglobulin M), used to localize the large subunit of RNA polymerase II (Bregman *et al.*, 1995), was a generous gift of Dr. Joe Gall (Carnegie Institution, Baltimore, MD). Lampbrush chromosome spreads were performed as previously described (Gall, 1998).

Confocal and Fluorescence Microscopy

Images were obtained using a Zeiss (Oberkochen, Germany) Axioplan microscope equipped with a Sony DXC-950P charge-coupled device camera and analySIS 2.1 software (SIS, Münster, Germany) or by confocal laser scanning microscopy (TCS NT system; Leica, Heidelberg, Germany). Fluorescent signals after double staining were recorded simultaneously at one scan using a dual-wavelength channel at 488 and 568 nm, no cross-talk was observed. All images were processed using Adobe Photoshop (Adobe Systems, Edinburgh, United Kingdom).

In Vivo RNA Label

Twenty-four hours before the labeling reaction, XTC cells at a concentration of 4×10^5 cells per well were seeded in a six-well tissue culture plate. Fifteen minutes before the labeling, cells were preincubated with 1 mM 2-deoxyadenosine, 1 mM tubercidine (7-deazaadenosine; Sigma), or 0.1 mM 5,6-dichloro-1-β-D-ribofuranosylbenzimidazole (DRB). One well remained untreated as a control. The labeling was done with 5 μCi of [U-^{14}C]uridine (5020 Ci/mmol; Amersham) and 20 μCi L-[methyl-^{3}H]methionine (77 Ci/mmol; Amersham) per well for 15 min in the presence or absence of the inhibitors listed above. Total RNA was isolated using TriStar reagent (AGS, Heidelberg, Germany), and poly(A)$^+$ RNA was purified on oligo(dT)-cellulose (QuickPrep Micro; Pharmacia Biotech) according to the instructions of the manufacturers. Poly(A)$^+$ and poly(A)$^-$ RNA were precipitated with trichloroacetic acid, and radioactive incorporation was monitored by scintillation counting.

```
        1                                                  50
xSAHH2  MSDKLSYKVA DISLADWGRK AIEIAENEMP GLMKMREMYS ESKPLKGARI
xSAHH1  MSDKLSYKVA DISLADWGRK AIEIAENEMP GLMKMREMHS ESKPLKGARI
mSAHH   MSDKLPYKVA DIGLAAWGRK ALDIAENEMP GLMRMREMYS ASKPLKGARI
rSAHH   MADKLPYKVA DIGLAAWGRK ALDIAENEMP GLMRMREMYS ASKPLKGARI
hSAHH   MSDKLPYKVA DIGLAAWGRK ALDIAENEMP GLMRMRERYS ASKPLKGARI
Consens M-DKL-YKVA DI-LA-WGRK A--IAENEMP GLM-MRE--S -SKPLKGARI

       51                                                 100
xSAHH2  AGCLHMTLQT AVLIETLTAI GAEVQWSSCN IFSTQDHAAA AIAKTGVPVY
xSAHH1  AGCLHMTLQT AVLIETLTAL GAEVQWSSCN IFSTQDHAAA AIAKTGVPVY
mSAHH   AGCLHMTVET AVLIETLVAL GAEVRWSSCN IFSTQDHAAA AIAKAGIPVF
rSAHH   AGCLHMTVET AVLIETLVAL GAEVRWSSCN IFSTQDHAAA AIAKAGIPVF
hSAHH   AGCLHMTVET AVLIETLVTL GAEVQWSSCN IFSTQDHAAA AIAKAGIPVY
Consens AGCLHMT--T AVLIETL--- GAEV-WSSCN IFSTQDHAAA AIAK-G-PV-

      101                                                 150
xSAHH2  AWKGETDEEY IWCIEQTIYF KDGKPLNMIL DDGGDLTNLV HTKYPQLLKG
xSAHH1  AWKGETDEEY IWCIEQTIYF KDGKPLNMIL DDGGDLTNLV HSKYPQLLKG
mSAHH   AWKGETDEEY LWCIEQTLHF KDG.PLNMIL DDGGDLTNLI HTKYPQLLSG
rSAHH   AWKGETDEEY LWCIEQTLHF KDG.PLNMIL DDGGDLTNLI HTKHPQLLSG
hSAHH   AWKGETDEEY LWCIEQTLYF KDG.PLNMIL DDGGDLTNLI HTKYPQLLPG
Consens AWKGETDEEY -WCIEQT--F KDG-PLNMIL DDGGDLTNL- H-K-PQLL-G

      151                                                 200
xSAHH2  IKGISEETTT GVHNLYKMKS SGTLQVPAIN VNDSVTKSKF DNLYGCRESL
xSAHH1  IKGISEETTT GVHNLYKMKS SGTLQVPAIN VNDSVTKSKF DNLYGCRESL
mSAHH   IRGISEETTT GVHNLYKMMS NGILNVPAIN VNDSVTKSKF DNLYGCRESL
rSAHH   IRGISEETTT GVHNLYKMMA NGILKVPAIN VNDSVTKSKF DNLYGCRESL
hSAHH   IRGISEETTT GVHNLYKMMA NGILKVPAIN VNDSVTKSKF DNLYGCRESL
Consens I-GISEETTT GVHNLYKM-- -G-L-VPAIN VNDSVTKSKF DNLYGCRESL

      201                                                 250
xSAHH2  IDGIKRATDV MIAGKVAVVA GYGDVGKGCA QALRAFGARV IITEIDPINA
xSAHH1  IDGIKRATDV MIAGKVAVVA GYGDVGKGCA QALRAFGARV IITEIDPINA
mSAHH   IDGIKRATDV MIAGKVAVVA GYGDVGKGCA QALRGFGARV IITEIDPINA
rSAHH   IDGIKRATDV MIAGKVAVVA GYGDVGKGCA QALRGFGARV IITEIDPINA
hSAHH   IDGIKRATDV MIAGKVAVVA GYGDVGKGCA QALRGFGARV IITEIDPINA
Consens IDGIKRATDV MIAGKVAV-A GYGDVGKGCA QALR-FGARV -ITEIDPINA
                                NAD+ binding site
      251                                                 300
xSAHH2  LQAAMEGYEV TTMDEASKEG NIFVTTTGCA DIVEGRHFEN MKDDSIVCNI
xSAHH1  LQAAMEGYEV TTMDEASKEG NIFVTTTGCA DIVEGRHFEN MKDDSIVCNI
mSAHH   LQAAMEGYEV TTMDEACKEG NIFVTTTGCV DIILGRHFEQ MKDDAIVCNI
rSAHH   LQAAMEGYEV TTMDEACKEG NIFVTTTGCV DIILGRHFEQ MKDDAIVCNI
hSAHH   LQAAMEGYEV TTMDEACQEG NIFVTTTGCI DIILGRHFEQ MKDDAIVCNI
Consens LQAAMEGYEV TTMDEA--EG NIFVTTTGC- DI--GRHFE- MKDD-IVCNI

      301                                                 350
xSAHH2  GHFDVELDVK WLNDNAAKKI NIKPQVDRYL LKNGRHIILL AEGRLVNLGC
xSAHH1  GHFDIELDVK WLNENAVKKV NIKPQVDRYL LKNGRHIILL AEGRLVNLGC
mSAHH   GHFDVEIDVK WLNENAVEKV NIKPQVDRYW LKNGRRIILL AEGRLVNLGC
rSAHH   GHFDVEIDVK WLNENAVEKV NIKPQVDRYL LKNGHRIILL AEGRLVNLGC
hSAHH   GHFDVEIDVK WLNENAVEKV NIKPQVDRYR LKNGRRIILL AEGRLVNLGC
Consens GHFD-E-DVK WLN-NA--K- NIKPQVDRY- LKNG--IILL AEGRLVNLGC

      351                                                 400
xSAHH2  AMGHPSFVMS NSFTNQVMAQ IELWTNTDKY PVGVYFLPKK LDEAVAAAHL
xSAHH1  AMGHPSFVMS NSFTNQVMAQ IELWTNTDKY PVGVYFLPKK LDEAVAAAHL
mSAHH   AMGHPSFVMS NSFTNQVMAQ IELWTHPDKY PVGVHFLPKK LDEAVAEAHL
rSAHH   AMGHPSFVMS NSFTNQVMAQ IELWTHPDKY PVGVHFLPKK LDEAVAEAHL
hSAHH   AMGHPSFVMS NSFTNQVMAQ IELWTHPDKY PVGVHFLPKK LDEAVAEAHL
Consens AMGHPSFVMS NSFTNQVMAQ IELWT--DKY PVGV-FLPKK LDEAVA-AHL

      401                                 433
xSAHH2  DKLGVKLTKL TDKQAKYLGL DKEGPFKPDH YRY
xSAHH1  DKLGVKLTKL TDKQAKYLGL DKEGPFKPDH YRY
mSAHH   GKLNVKLTKL TEKQAQYLGM PINGPFKPDH YRY
rSAHH   GKLNVKLTKL TEKQAQYLGM PINGPFKPDH YRY
hSAHH   GKLNVKLTKL TEKQAQYLGM SCDGPFKPDH YRY
Consens -KL-VKLTKL T-KQA-YLG- ---GPFKPDH YRY
```

Figure 1. Protein sequence alignment of vertebrate SAHH. The cDNA-derived amino acid sequences of *X. laevis* (xSAHH 1, GenBank accession number [gb] L35559 and this communication; xSAHH 2, gb AJ007835 and this communication), mouse (mSAHH, gb L32836), rat (rSAHH, gb M15185) and human (hSAHH, gb M61832) have been aligned together with the consensus sequence, using the GCG programs Pileup and Pretty. The two isoforms of *X. laevis* are distinguished from one another by eight conservative changes, each marked by shading. Sequences obtained by protein microsequencing of tryptic peptides of the *X. laevis* oocyte protein are underlined in xSAHH. Lysine and arginine residues are shown in bold. The NAD^+ binding site is printed in italics and underlined in the consensus. An amphiphatic helical domain near the C terminus is underlined twice, and a lysine residue (K^{427}) shown to be essential for tetramer formation and for catalytic activity of the hSAHH (Ault-Riche *et al.*, 1994) is printed in italics and shaded.

RESULTS

The Maternal Nuclear Antigen of mAb 32-5B6 Is the Enzyme xSAHH

To identify the maternal nuclear antigen of the mAb 32-5B6 (Dreyer *et al.*, 1981), we have screened an expression library containing cDNA of *X. laevis* oocytes, unidirectionally inserted in a λ Uni-zap XR vector, by means of the mAb. Of $\sim 5 \times 10^5$ phage plaques analyzed, 6 expressed a polypeptide that was bound by the mAb. Five of the six phage colonies were purified, and the plasmid was excised in vivo and sequenced. All of the five independently isolated clones contained cDNA encoding the enzyme SAHH (M_r 47,000; EC 3.3.1.1). Clone 1 encodes a polypeptide identical to the previously published xSAHH (Seery *et al.*, 1994). The other four cDNAs encode a closely related polypeptide that is 98% identical at the amino acid level to the known xSAHH and most likely represents a second form of the enzyme that was to be expected because of the pseudotetraploid genome of *X. laevis*. We have therefore referred to the two forms as xSAHH 1 and 2 (Figure 1).

To verify that the enzyme xSAHH is the antigen of mAb 32-5B6, we separated oocyte nuclear proteins by two-dimensional gel electrophoresis as described previously (Dreyer and Hausen, 1983) and excised the antigen-containing area. The mAb binds to two polypeptides with a molecular mass of apparently 46 kDa with slightly different isoelectric points (Dreyer and Hausen, 1983). Material containing both polypeptides was pooled from 14 gels, and tryptic peptides were purified and processed for microsequencing as detailed in MATERIALS AND METHODS. Eight tryptic peptides were fully or partially sequenced, and all of the resulting sequence information conformed to peptides found in the cDNA-deduced sequence of xSAHH C-terminally adjacent to a lysine or arginine residue. Peptide sequencing resulted in a total of 90 amino acids that are underlined in Figure 1. The difference in the primary amino acid sequence between the two isoforms, consisting of eight conservative changes, did not lead to ambiguities in the peptide sequences. The two isoforms of the antigen of mAb 32-5B6 differ on two-dimensional gels in their isoelectric point by ~0.1 (Dreyer and Hausen, 1983), and the calculated IPs of the cDNA-deduced polypeptides are 6.44 and 6.36, showing that xSAHH2 is the more acidic form. In conclusion, direct protein sequencing and cDNA cloning showed unequivocally that xSAHH is the antigen bound by mAb 32-5B6. SAHH is active as a tetramer, and both isoforms are likely to function equivalently, because they differ by only a few conservative changes (Figure 1).

Is Nuclear xSAHH Associated with CpG Methylation of DNA?

Nuclear SAM-dependent methylation reactions that could profit from a nuclear localization of SAHH are methylation of DNA at CpG dinucleotides, cap methylation of mRNA, internal methylation of rRNA, and protein methylation. In somatic cells, DNA methylation mainly serves to maintain a preestablished pattern of CpG methylation, and maintenance methylation is closely linked to DNA replication during S phase, because the DNA methyltransferase has a strong preference for hemimethylated DNA at the replication forks (Bestor, 1992; Araujo *et al.*, 1998).

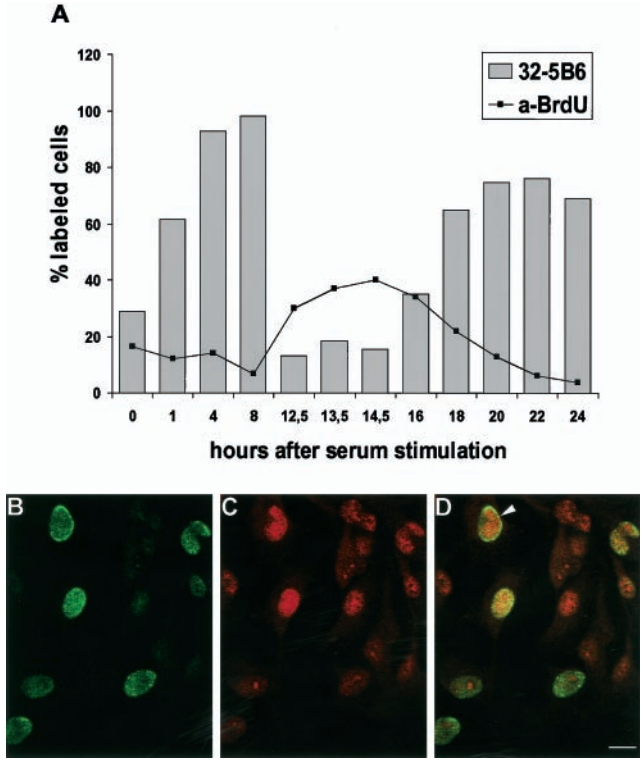

Figure 2. The amount of nuclear xSAHH in XTC cells is dependent on the cell cycle. (A) XTC cells arrested in G0 by serum starvation were stimulated to exit G0 by addition of 10% serum. Cells were pulse labeled with BrdU 1 h before fixation, and parallel samples were immunostained for BrdU incorporated in DNA and for xSAHH. The percentage of significant nuclear staining is plotted against the time after serum stimulation (not drawn to scale). (B–D) Nonsynchronous XTC cells were pulse labeled for 1 h with BrdU, fixed, and double stained for de novo–synthesized DNA (B) and for xSAHH (C). Superposition of confocal images shows limited coincidence of both labels (D). The example shown was selected for maximal overlap of both labels. In the nucleus marked with an arrowhead, the peripheral BrdU label likely represents replicating heterochromatin. Bar, 10 μm.

In asynchronous A6 cells, the xSAHH antigen is found in almost all cell nuclei, yet the intensity of staining varies between cells (see Figure 7A). To investigate whether the nuclear localization of xSAHH is dependent on the cell cycle, XTC tissue culture cells were arrested in G0 by serum starvation and were released and synchronized by readdition of serum. The XTC cells were pulse labeled with BrdU before fixation and stained for incorporated BrdU and for xSAHH (Figure 2A). Immunofluorescent staining was low in quiescent cells after serum starvation. The percentage of cells with significant nuclear staining for xSAHH increased 1 h after release from serum starvation, and this percentage and the staining intensity increased further during subsequent hours. The onset of S phase was accompanied by a significant decrease in nuclear xSAHH. Throughout S phase, lasting from ~12 to 18 h after serum stimulation, both the percentage of stained nuclei and the intensity of staining for xSAHH remained low. Subsequently, incorporation of BrdU decreased and the amount of xSAHH found in the nucleus

increased again. The mitotic index increased significantly after 22 h. This time course indicates that nuclear accumulation of xSAHH is higher in G1 and G2 than in S phase, and it argues against the notion that DNA methylation is the primary reaction associated with the presence of xSAHH in the nucleus. Nevertheless, the presence of SAHH in the replication forks could enhance the efficiency of DNA methylation by instantaneous hydrolysis of S-adenosylhomocysteine. To investigate whether xSAHH was localized on replicating chromatin, nonsynchronous XTC cells were labeled with BrdU for 1 h, fixed, and double stained for incorporated BrdU (Figure 2B) and for xSAHH (Figure 2C). Thin optical sections generated by means of a confocal laser scanning microscope are shown, and superposition of both images in Figure 2D clearly shows that not all of the nuclei in S phase contain high amounts of xSAHH, whereas some nuclei without BrdU label do contain xSAHH. One nucleus labeled with an arrowhead in Figure 2D shows noncongruence of both labels. The peripheral BrdU label likely represents replicating heterochromatin known to replicate later than the euchromatin (Rizzoli *et al.*, 1992; Breschi *et al.*, 1998; Mazzotti *et al.*, 1998), whereas xSAHH prevails in the center of the nucleus, potentially near already replicated chromatin. Alternatively, the absence of xSAHH from replicating heterochromatin could be due to the fact that CpG islands found in the heterochromatin remain unmethylated (Bird, 1986). In conclusion, the presence of xSAHH in the nucleus is clearly not restricted to S phase.

In contrast to differentiated cells, whose methylation pattern is copied to the daughter cells, the DNA methylation pattern in embryogenesis is highly dynamic (Monk *et al.*, 1987). This has primarily been studied in the mouse, where the gamete-specific methylation pattern is first erased, before a global remethylation occurs, with the exception of the CpG islands. Cell differentiation is thought to be accompanied by a selective gene-specific demethylation, leading to transcriptional activation of specific genes (Heby, 1995).

To investigate whether the regulated nuclear accumulation of xSAHH in embryogenesis correlates with the pattern of methylation, we have determined the content of methylated CpG in total DNA of *Xenopus* embryos between blastula and late neurula. As shown by nearest neighbor analysis, the percentage of methylated CpG decreases significantly during the phase of nuclear translocation of xSAHH in the embryo (Table 1). At blastula stage 9, when xSAHH is still mainly cytoplasmic, ~80% of CpG is methylated. By the end of gastrulation (stage 12.5), when xSAHH is found in most nuclei, only 25% of the CpG is methylated. Methylation decreases further to 13% by the late neurula stage 20 (Table 1). In conclusion, nuclear translocation of xSAHH in embryogenesis is not temporally linked to de novo methylation of DNA. In parallel experiments, embryos were injected 1 h before isolation of the DNA with the nucleoside homologue DMA, which is known to specifically inhibit SAHH and therefore indirectly DNA methyltransferase (Bergmann *et al.*, 1994). This treatment reduces the content of methylated CpG from 81 to 15% at stage 9 (Table 1), indicating that the results obtained by nearest neighbor analysis are indeed dependent on ongoing methylation.

Table 1. Content of 5-methyl cytosine (m^5C) in DNA of embryos of different stages

Embryo stage	% m^5C[a]
9 (blastula)	81 ± 5
9 (1 h after DMA)	15
9.5 (late blastula)	67 ± 7
12.5 (late gastrula)	25 ± 5
20 (late neurula)	13

[a] The analysis was performed two to five times per time point.

Nuclear Localization of xSAHH Coincides with mRNA Synthesis

After 12 rapid and synchronous cell divisions without zygotic gene expression, cell division becomes asynchronous after the midblastula transition (MBT) at stage 8.0, and mRNA synthesis gradually increases (Newport and Kirschner, 1982a,b). Because mRNA synthesis and nuclear translocation of xSAHH both increase after the MBT, we have reinvestigated the intracellular localization of xSAHH in embryogenesis by whole-mount staining with mAb 32-5B6 and subsequent immunofluorescent analysis of glycolmethacrylate sections, resulting in a higher resolution when compared with the wax sections used before (Dreyer *et al.*, 1982).

Up to late blastula stage 9, xSAHH is mainly localized in the cytoplasm and at the cell borders (Figure 3A), although nuclear accumulation with simultaneous cytoplasmic depletion is seen in single cells (Figure 3A, arrowhead). This is more frequently seen during gastrula stages 10 and 10.5, and examples are indicated by arrowheads in Figure 3, E and G. Although excluded from interphase nuclei, xSAHH is found in the yolk-free zone surrounding the condensed chromosomes during mitosis. This perichromosomal localization is seen from prometaphase to telophase, and it is not accompanied by cytoplasmic depletion of the antigen. (Figure 3, A--D, arrows). After stage 9, the nucleus and cytoplasm are both stained, and the nuclear accumulation of the antigen gradually increases (Figure 3, C–G). Nuclear localization in most cells is first seen in the mesoderm of the marginal zone and in the endoderm. The intracellular localization of xSAHH remains, however, heterogeneous throughout gastrulation, with no preference for the prospective dorsal or ventral region of the embryo detectable on serial sections of the type shown in Figure 3K. Because the cell cycle lengthens and becomes asynchronous after the MBT, the patchy overall pattern seen in Figure 3, E, G, I, and K, might reflect the heterogeneity of the individual cells with respect to the cell cycle. Subsequently the percentage of interphase nuclei with significant xSAHH staining gradually increases, until the antigen is detected in virtually all nuclei at the end of gastrulation (Figure 3I). Cells that accumulate xSAHH in the nucleus simultaneously lose it from the cytoplasm; therefore, the increase in nuclear xSAHH is not necessarily dependent on de novo synthesis. Zygotic transcription of the xSAHH gene has been reported to start at late tail bud stage 27 (Seery *et al.*, 1994). The maternal antigen persists throughout embryogenesis (Dreyer *et al.*, 1982), and de novo protein synthesis of the antigen of mAb 32-5B6 was not detected in

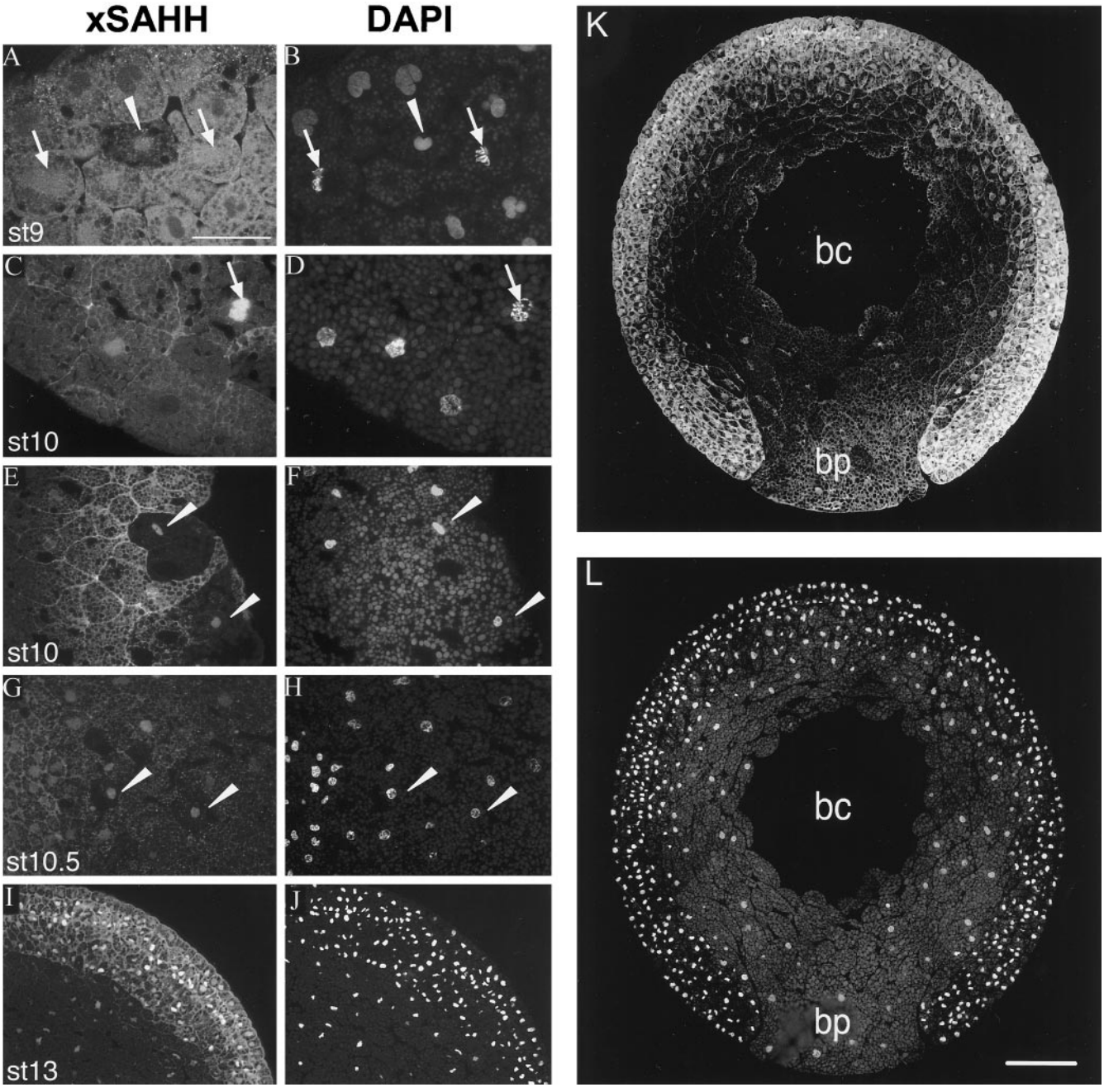

Figure 3. xSAHH translocates into interphase nuclei during gastrulation. Intracellular localization of endogenous xSAHH was analyzed on Technovit sections after whole-mount immunofluoresescent staining using mAb 32-5B6 (A, C, E, G, I, and K), and counterstaining of the same sections for DNA with DAPI is shown in B, D, F, H, J, and L. Details of sections cut in the animal to vegetal direction were selected that show the marginal zone of a late blastula at stage 9 (A and B), the vegetal area (C and D), and the dorsal lip of an early gastrula at stage 10 (E and F), a marginal area of a gastrula at stage 10.5, with mesoderm to the left and endoderm to the right (G and H), and all three germ layers anteriorly of a very early neurula at stage 13 (I and J). Single interphase nuclei showing nuclear xSAHH are marked with arrowheads in A–H. Mitotic cells are marked with arrows, and arrows point at prometaphase in C and D. On a complete transverse section of a gastrula at stage 11.5 (K) the endoderm of the blastoporus (bp) is flanked by the two blastoporal lips, containing mesoderm and ectoderm. bc, remnant of the blastocoel. Cytoplasmic xSAHH is excluded from yolk platelets and is concentrated at the cell boundaries. Bars: A–J, 50 μm; L, 200 μm. Sections were 2 μm thick in G and H and 5 μm thick in all other panels.

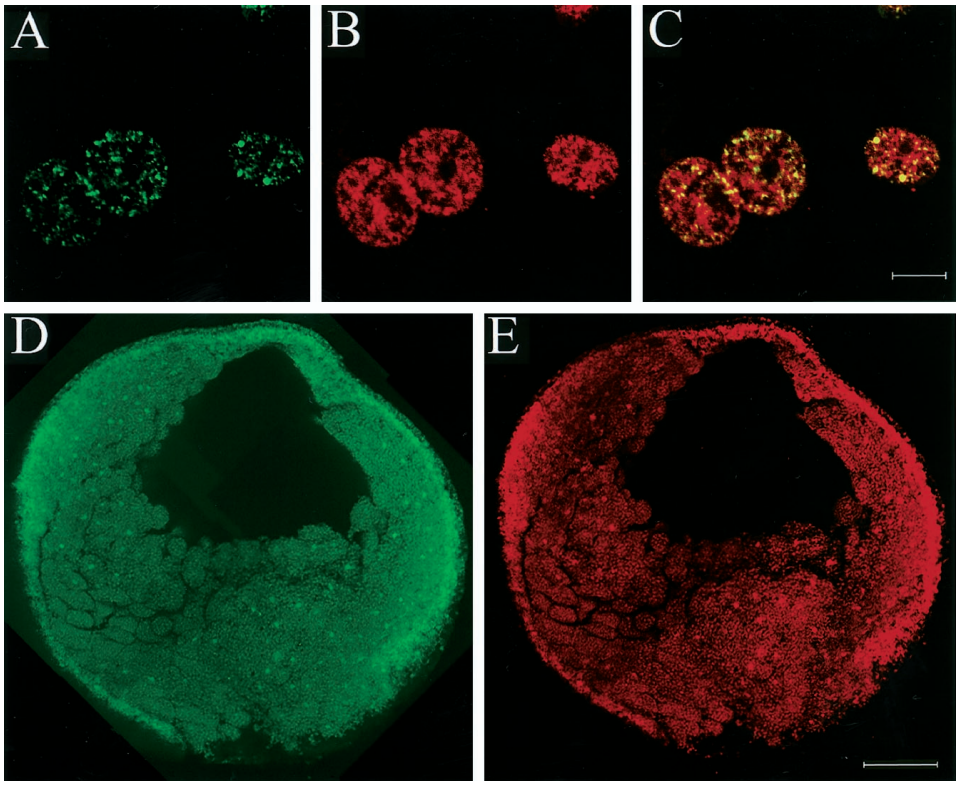

Figure 4. Nuclear run-on transcriptional assay in A6 cells and embryos. Transcriptional activity was monitored by a nuclear run-on assay with incorporation of Br-UTP in permeabilized A6 cells (A) and in embryos (D), as detailed in MATERIALS AND METHODS. A6 cells were fixed after 10 min of labeling and double stained for incorporated Br-UTP (A), and xSAHH (B). The confocal images shown in A and B are superimposed in C. Bar, 10 μm. (D and E) A midgastrula embryo at stage 10.5 was coinjected with digitonin and ribonucleotides including Br-UTP and fixed after 60 min of labeling at stage 11. The gastrula was dissected in halves along the animal to vegetal axis, and halves were double stained as whole mounts for the Br-UTP label and for xSAHH. Confocal images of the surface show coincident nuclear staining with anti BrU (D) and with mAb 32-5B6 for xSAHH (E). Bar, 200 μm.

significant amounts up to stage 36 (Dreyer and Hausen, 1983), indicating that it is essentially the maternal protein pool of xSAHH that changes its intracellular localization during embryogenesis. As a consequence of the distribution of the maternal nuclear protein in mainly the animal hemisphere during oocyte maturation (Hausen *et al.*, 1985), the total concentration of the antigen remains higher in the mesoderm and ectoderm compared with the endoderm, as demonstrated in Figure 3, G, I, and K.

The MBT is not accompanied by a sudden translocation of xSAHH to the nuclei of the embryo. Our immunohistological observation of a gradual nuclear translocation of xSAHH during gastrulation suggests that nuclear accumulation of xSAHH coincides in time and space with the increase of zygotic mRNA synthesis. A detailed autoradiographic analysis has previously shown that mRNA synthesis starts simultaneously in the whole mesoderm and ectoderm between stages 8.5 and 9. In the ectoderm, a moderate and transient transcriptional activation was observed before gastrulation, followed by silencing between stages 10 and 10.5, and a subsequent full activation, achieved at stage 13, when neurulation begins (Bachvarova and Davidson, 1966).

Recent evidence suggests that RNA (guanine-7)-methyltransferase is bound to the phosphorylated C-terminal domain of the large subunit of RNA polymerase II in the transcriptional elongation complex (McCracken *et al.*, 1997). A close association of SAHH to this complex in the nucleus could aid transcription by preventing product inhibition of RNA (guanine-7)-methyltransferase. As a first step to investigate whether xSAHH colocalizes to transcriptionally active RNA polymerase II, a nuclear run-on assay to detect RNA polymerase II transcripts (Jackson *et al.*, 1993; Wansink *et al.*, 1993) was performed in A6 cells (Figure 4, A–C). The subsequent immunodetection of incorporated Br-UTP in nascent mRNA (Figure 4A) and of endogenous xSAHH (Figure 4B) was performed with a confocal laser scanning microscope. As seen at the light microscope level, xSAHH is found in fine nuclear granules, excluding the nucleoli (see Figure 7A). The confocal optical section shown in Figure 4B shows this at higher resolution, and superposition with the pattern of incorporated Br-UTP (Figure 4C) shows that all nascent mRNA colocalizes to nuclear areas abundant in xSAHH, although the enzyme is more widely distributed (Figure 4C). In the presence of low doses of α-amanitin, no significant extranucleolar Br-UTP label was detected, indicating that the labeled RNA detected in this assay was transcribed by RNA polymerase II.

To correlate the onset of zygotic transcription in the embryo with the nuclear translocation of SAHH, a nuclear run-on transcription assay was performed in whole embryos at gastrula stages by coinjection of Br-UTP and digitonin to permeabilize the cells. After incubation for 60 min, embryos were fixed and double stained for incorporated Br-UTP and xSAHH as detailed in MATERIALS AND METHODS. Colocalization of de novo–synthesized RNA and xSAHH was frequently seen in cell nuclei at gastrula stage 11 (Figure 4, D and E).

Immunohistology also demonstrates that xSAHH is a predominantly nuclear enzyme in cells with high transcriptional activity (Wedlich and Dreyer, 1988; see DISCUSSION). It is not found in the transcriptionally silenced nuclei

of erythrocytes or male germ cells. In testes, nuclear xSAHH is most abundant in the highly transcriptionally active Sertoli cells. In addition, other somatic cells and the spermatogonia contain significant amounts of nuclear xSAHH (Figure 5, A and B). Subsequently, the synchronously differentiating spermatocytes lose the nuclear xSAHH at the same time as transcriptional silencing occurs (Figure 5, A and B). In the nucleus of the early diplotene oocyte xSAHH accumulates in the vicinity of the lampbrush chromosomes, whereas it is excluded from the center of the nucleoli, with some accumulation around the nucleolar periphery (Figure 5, C and E). The localization of xSAHH in the oocyte nucleus is similar to, yet more diffuse than, that of RNA polymerase II. We have compared the localization of both enzymes on adjacent frozen sections using the mAbs H14 against RNA polymerase II (Figure 5G) and mAb 32-5B6 (Figure 5E). Whereas RNA polymerase II is highly concentrated at the loops of the transcriptionally active lampbrush chromosomes (Gall and Murphy, 1998; Figure 5G), xSAHH is more diffusely distributed throughout the nucleus (Figure 5E). However, to analyze a possible colocalization of a subfraction of xSAHH with RNA polymerase II, spreads of lampbrush chromosomes were double stained for xSAHH and for RNA polymerase II and analyzed by confocal laser scanning microscopy (Figure 5, I–K). Here, xSAHH is found on all loops representing actively transcribed genes (Figure 5I). The localization of the subfraction of xSAHH seen on spreads of lampbrush chromosomes (Figure 5I) is identical to that of RNA polymerase II (Figure 5J) as is shown by superposition of both confocal optical sections (Figure 5K). In conclusion, there is ample evidence for a nuclear accumulation of xSAHH in cells with a high rate of mRNA synthesis.

xSAHH Activity Is Required for Methylation and Synthesis of pre-mRNA

The prevalence of nuclear accumulation of xSAHH in transcriptionally active cells suggests a supporting role of xSAHH in methylation of RNA or heterogeneous nuclear ribonucleoprotein. To investigate whether SAHH activity is required for efficient cap methylation and synthesis of heterogeneous nuclear RNA (hnRNA), we have labeled *Xenopus* tissue culture cells (XTC) simultaneously with [U-^{14}C]uridine and L-[methyl-^{3}H] methionine in the presence or absence of inhibitors of SAHH (Figure 6). In control experiments without inhibitors, ~80% of the incorporated [U-^{14}C]uridine was found in the poly(A)$^+$ fraction of the RNA after a pulse of 15 min, whereas ~70% of the [^{3}H]methyl label was found in the poly(A)$^-$ fraction. Labeling of the poly(A)$^+$ RNA was sensitive to DRB, as expected for polymerase II transcripts. The amount of [^{3}H]CH_3 incorporated in poly(A)$^+$ RNA was reduced in the presence of inhibitors of SAHH, probably because of product inhibition of methyl transferase by *S*-adenosylhomocysteine. Of the two inhibitors applied, tubercidine was previously reported to be the more potent inhibitor of SAHH (Fabianowska-Majewska *et al.*, 1994), and accordingly it inhibited incorporation of [^{3}H]CH_3 into poly(A)$^+$ RNA by 76%, whereas 2-deoxyadenosine inhibited methylation by only 45%. Simultaneously, [U-^{14}C]uridine labeling of poly(A)$^+$ RNA was inhibited by 86 and 63%, respectively, indicating that transcriptional elongation by RNA polymerase II is dependent on cap methylation (Figure 6). In conclusion, nuclear cap methylation of hnRNA depends on SAHH activity and is itself a prerequisite of efficient transcriptional elongation.

Nuclear Localization of xSAHH Requires the C Terminus and the N Terminus

SAHH has previously not been described as a nuclear enzyme, and no obvious bona fide nuclear localization signal is found in the cDNA-deduced primary amino acid sequences of SAHH, although most of the basic amino acids are conserved between the mammalian and the *Xenopus* sequences (Figure 1). As a tetramer of 180 kDa, xSAHH cannot be expected to translocate to the nucleus by diffusion.

The endogenous xSAHH is essentially nucleoplasmic during interphase in *Xenopus* A6 cells, as revealed by staining with mAb 32-5B6 (Figure 7A). To prove that the translation product of the xSAHH cDNA can translocate to the cell nucleus, we have transfected different cell lines with cDNA encoding MT-xSAHH. In the *Xenopus* cell line A6 (Figure 7, B and C) the exogenous protein MT-xSAHH was predominantly nuclear in ~50–90% of the transfected cells. The percentage of cells with predominantly nuclear localization of MT-xSAHH increased with the time after transfection, and 120 h after transfection nuclear localization was seen in ~90% of the transfected cells (Figure 7B).

To assess which parts of the polypeptide are indispensable for nuclear translocation, we have deleted parts of the cDNA before transfection (Figure 8B). When the nine C-terminal amino acids were replaced by the six amino acids LEPLEL encoded by the vector, the resulting protein MT-xSAHHΔ425–433 rarely localized exclusively to the nucleus of transfected A6-cells (Figures 7D and 8A). A frame shift mutation resulting in the replacement of the 32 C-terminal aa of xSAHH did not aggravate this phenotype (Figures 7E and 8A). This demonstrates that replacing the C-terminal 9–32 aa significantly reduced but did not preclude nuclear translocation of xSAHH in *Xenopus* A6 cells.

Because replacement of the 32 C-terminal amino acids reduced but did not prevent nuclear translocation, we tested the influence of a more extensive C-terminal deletion, xSAHHΔ361–433, which completely removed a conserved, putative, amphiphatic α-helical domain (Figures 1 and 8B). Transfected cells could not accumulate this protein in the nucleus. In >50% of the cells the antigen was excluded from the nucleus (Figures 7F and 8A).

Interestingly, replacement of the 13 N-terminal amino acids of the MT-xSAHH protein by linker sequences inhibited nuclear accumulation of the fusion protein almost completely (Figures 7G and 8A), and replacement of the N-terminal 21 aa rendered nuclear accumulation impossible (Figures 7H and 8A). In conclusion, the N terminus of xSAHH, which forms a conserved α-helical domain, is indispensable for nuclear translocation. Nevertheless, C-terminal truncations also affected the intracellular localization, and therefore nuclear accumulation of the xSAHH protein cannot be attributed to a single linear motif within its sequence.

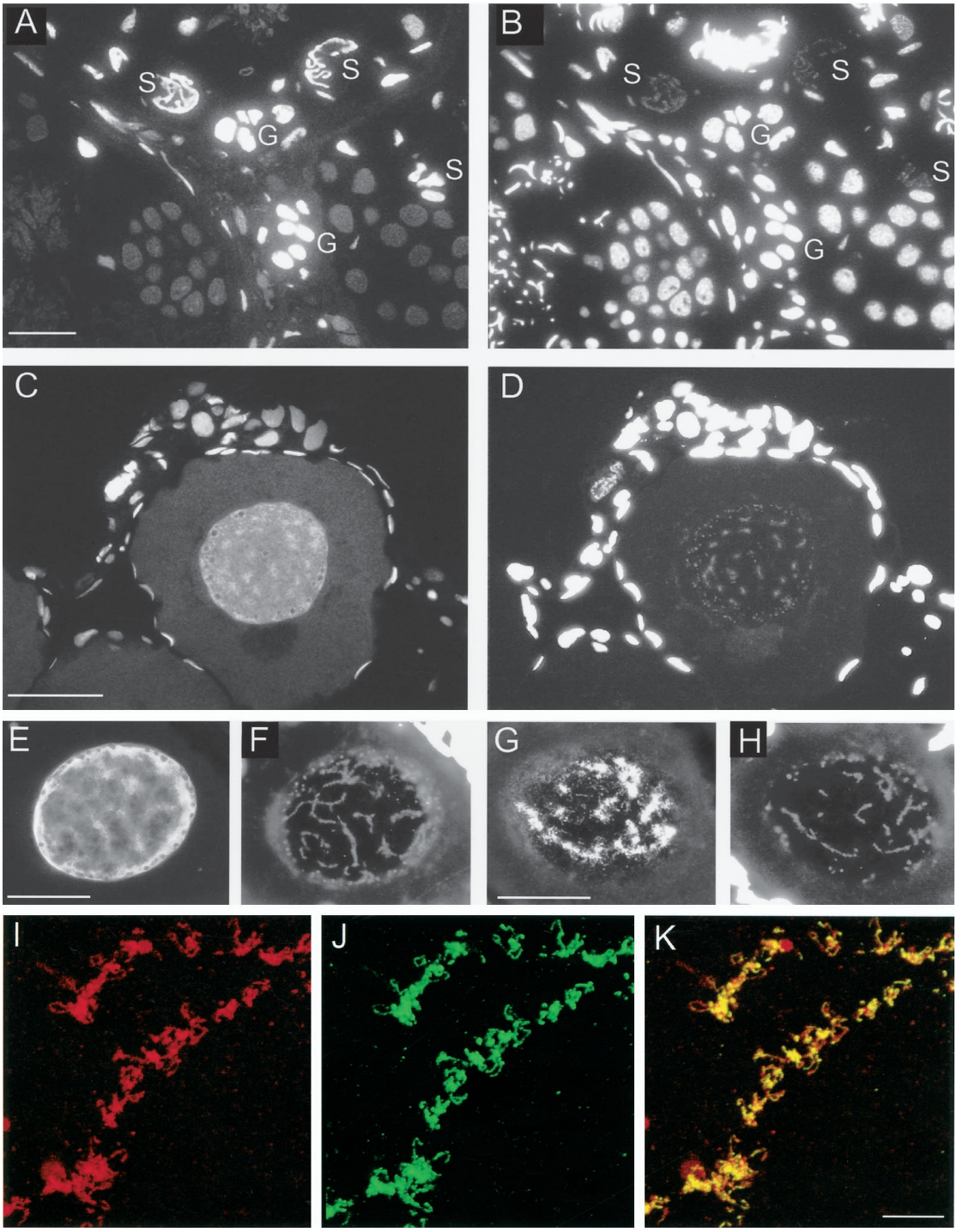

Figure 5. Immunohistological localization of xSAHH in the nuclei of germ cells. xSAHH was detected on 1.5-μm thin sections after whole-mount immunofluorescent staining of adult testis (A) and ovary from a 4-cm-long young female (C) with mAb 32-5B6. (B and D) Counterstaining of the same sections with DAPI. In the testis (A and B), nuclear staining with 32-5B6 predominates in transcriptionally active Sertoli cells (S) and spermatogonia (G). In the ovary (C and D), xSAHH is nuclear in all cells. In the single diplotene (stage I) oocyte nucleus shown, the xSAHH antigen appears most highly concentrated around the lampbrush chromosomes, which are weakly stained with DAPI in D. (E–H) Frozen sections of an ovary were stained with mAb 32-5B6 (E) and with anti-RNA Polymerase II mAb H14 (G). (F and H) DAPI counterstain of the sections shown in E and G. Follicle cell nuclei stained with DAPI are overexposed in D, F, and H to visualize lampbrush chromosomes. Bar, 50 μm. (I–K) Lampbrush chromosome spread from a stage V oocyte double stained for xSAHH (I) and for RNA polymerase II (J). The confocal images shown in I and J are superimposed in K. Bar in K, 10 μm.

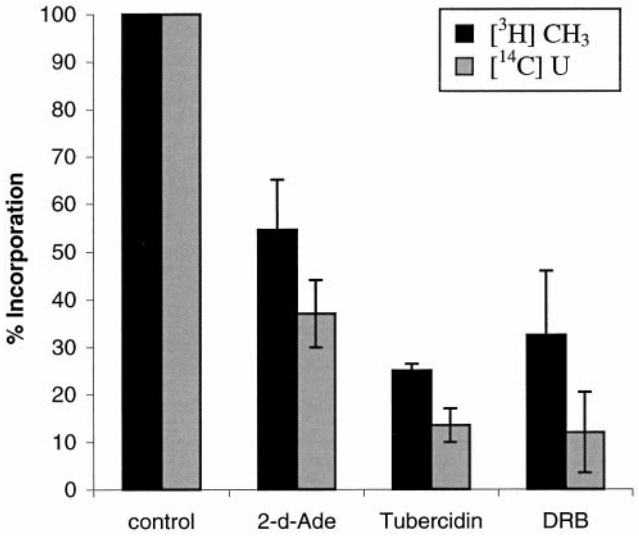

Figure 6. Inhibitors of SAHH interfere with methylation and elongation of poly(A)$^+$ RNA. XTC cells were simultaneously pulse labeled with L-[methyl-^{3}H]methionine and [U-^{14}C]uridine in the presence or absence of 2-deoxyadenosine (2dAde), tubercidine, or DRB, and the incorporation of radioactive precursors in poly(A)$^+$ RNA was analyzed as detailed in MATERIALS AND METHODS. The results of two independent experiments are combined and shown with error bars. Incorporation of [U-^{14}C]uridine in poly(A)$^+$ RNA of control cells was between 290 and 373 cpm, and incorporation of [^{3}H]methyl was between 30 and 74 cpm.

DISCUSSION

xSAHH Is a Conditionally Nuclear Enzyme

Based on biochemical cell fractionation experiments and because of its role in intermediate metabolism, SAHH has previously been regarded as a predominantly cytoplasmic enzyme (Hershfield and Krodich, 1978; Turner *et al.*, 1997). Surprisingly, the antigen concentration of xSAHH is higher in the nucleus than in the cytoplasm in oocytes, in embryos after gastrulation, and in many differentiated cell types. In embryos at cleavage and early blastula, xSAHH is predominantly cytoplasmic and cannot be shifted into the nuclei by artificially extending the cell cycle (Dreyer, 1987). In tissue culture cells, the nuclear concentration of xSAHH is dependent on the physiological state of the cell. SAHH is a highly conserved, ubiquitous, essential enzyme, and its activity is indispensable for SAM-dependent methyltransferases, because an accumulation of the byproduct *S*-adenosylhomocysteine causes product inhibition. Deletion of the SAHH gene in mouse embryos leads to early embryonic lethality (Miller *et al.*, 1994).

SAM-dependent methylation takes place in the cytoplasm, on membranes, and in the nucleus and possibly other cellular compartments. Hydrolysis of *S*-adenosylhomocysteine could be achieved in the cytoplasm, because this substrate should be able to diffuse freely between compartments because of its low molecular weight. Alternatively, the enzyme SAHH could have access to the different compartments of the cell, resulting in a close proximity of SAHH to methyltransferases that is likely to enhance the efficiency of methylation reactions.

Nuclear Localization of xSAHH Is Linked to Transcriptional Activity

Because of the notion that a close spatial association of SAHH to methyltransferase might enhance methylation processes, we have investigated whether SAM-dependent nuclear methylation reactions correlate to the presence of xSAHH in the nucleus. The observed net demethylation of CpG dinucleotides during embryogenesis (Table 1) conforms to the observation that promoter-specific demethylation begins after the MBT (Matsuo *et al.*, 1998). Furthermore, a demethylation of specific sequences within the untranscribed spacer of the rRNA genes has previously been described to begin at the onset of rRNA synthesis, at stage 10 (Bird *et al.*, 1981a,b). Because overt nuclear translocation of xSAHH begins at late blastula and proceeds gradually during gastrulation, there is no apparent temporal correlation to de novo methylation, which most probably occurs at a later developmental stage, during organogenesis. Nevertheless, a functional link between SAHH activity and DNA methylation becomes obvious, because inhibition of SAHH by DMA reduces the content of methylated CpG on DNA (Table 1). Therefore, a minor amount of nuclear xSAHH might be sufficient to hydrolyze *S*-adenosylhomocysteine produced by DNA methylation, whereas most of the enzyme is still cytoplasmic. Alternatively, hydrolysis of *S*-adenosylhomocysteine could occur in the cytoplasm during cleavage and blastula stages. For thermodynamic reasons demethylation of DNA requires a pathway that is distinct from a reversal of the methylation reaction, and therefore it is unlikely that xSAHH plays a role during net demethylation of the embryonic DNA (Cooper *et al.*, 1983; Kirillov *et al.*, 1996; Matsuo *et al.*, 1998).

Nuclear accumulation of xSAHH in embryogenesis does, however, correlate with a significant increase in transcriptional activity after the MBT (Newport and Kirschner, 1982a,b). All enzymes and their cofactors required for mRNA synthesis and processing might be expected to be present in the nucleus at the onset of zygotic transcription. However, RNA polymerase II is present in all nuclei of the embryo at blastula stages, and its presence obviously precedes that of xSAHH (our unpublished results). Probably the intracellular distribution of xSAHH differs from that of the RNA polymerase II because the function of RNA polymerase II is restricted to the nuclear compartment, whereas xSAHH is active in the cytoplasm as well. The predominant nuclear localization of the xSAHH antigen in G1 and G2 phase in *Xenopus* tissue culture cells and nuclear run-on assays show a temporal and spatial correlation between transcriptional activity and xSAHH in the nucleus. A fraction of xSAHH, found on lampbrush chromosome spreads, colocalizes with RNA polymerase II on the transcriptionally active loops (Figure 5, I–K). In ovary sections, however, xSAHH is more diffusely localized to the vicinity of the chromosomes compared with the pattern of RNA-polymerase II (Gall and Murphy, 1998; Figure 5, C–H); therefore a strong and exclusive binding of xSAHH to RNA-polymerase II is unlikely.

From a number of immunohistological observations we have gathered evidence for a prevalent nuclear localization of xSAHH in transcriptionally active cells: secretory cells of the cement gland, of the pharyngobranchial tract (Dreyer,

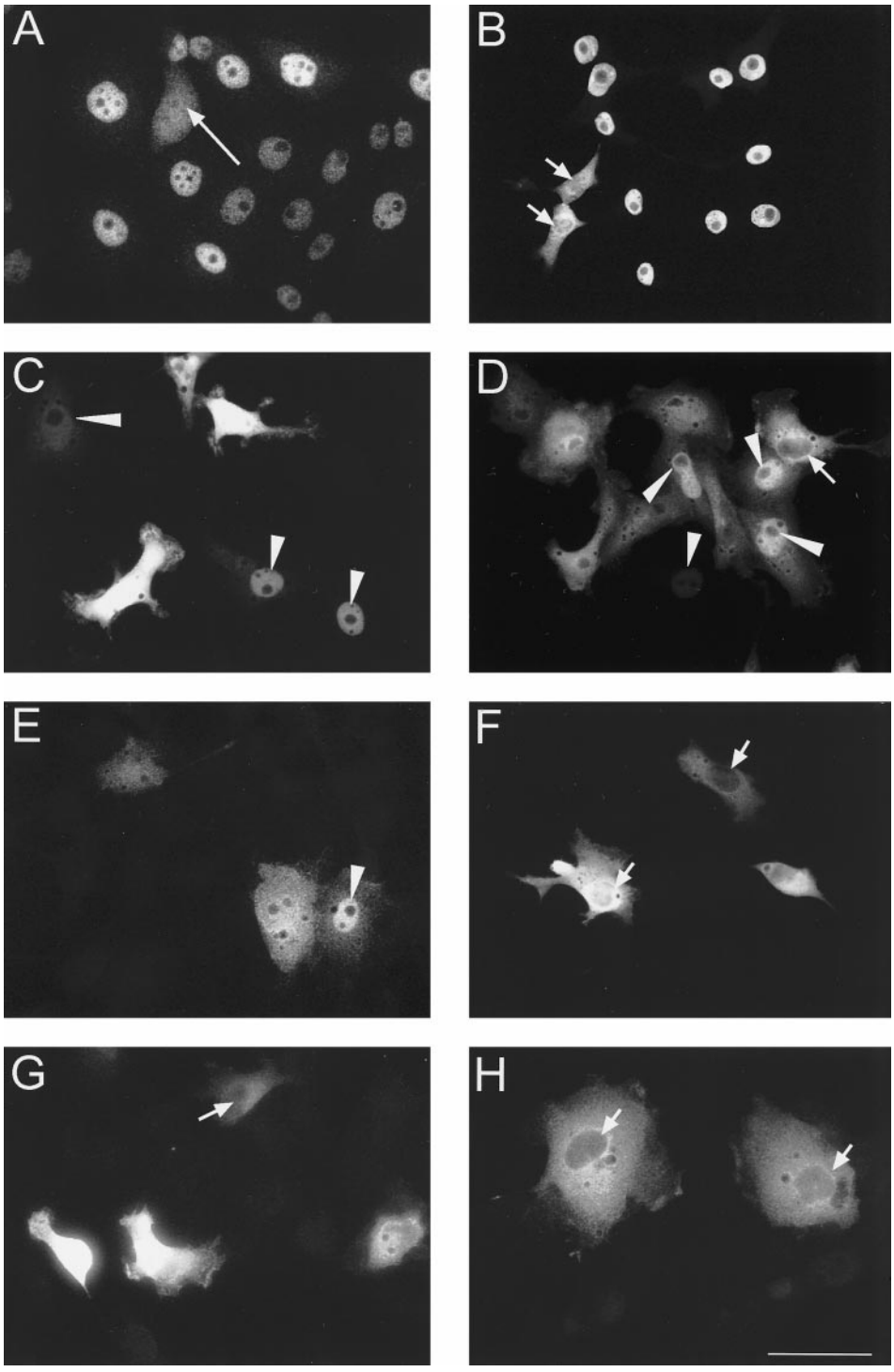

Figure 7. Nuclear translocation of full-length and mutated xSAHH in transfected cells. (A) Endogenous nucleoplasmic xSAHH stained with mAb 32-5B6 in untransfected A6 cells. A mitotic cell is marked by a long arrow. Full-length (B and C) and C-terminally (D-F) and N-terminally deleted (G and H) MT-xSAHH was detected in *Xenopus* A6 cells using mAb 9E10 after transient transfection as detailed in MATERIALS AND METHODS. Cells were fixed and processed for immunofluorescence 120 h (B) or 40–48 h (C–H) after transfection. Cells were transfected with pCS2+MT containing cDNA encoding full-length xSAHH (B and C), xSAHHΔ425–433 (D), xSAHHΔ402–433 (E), xSAHHΔ361–433 (F), xSAHHΔ1–13 (G), or xSAHHΔ1–21(H). Transfected cells with predominantly nuclear localization of MT-xSAHH are marked with arrowheads, and cells with predominantly cytoplasmic localization are marked with short arrows. Bar, 50 μm.

1989), of the exocrine pancreas and of the differentiated gut epithelium (Wedlich and Dreyer, 1988), as well as transcriptionally active Sertoli cells show intense nuclear staining with mAb 32-5B6. Conversely, nuclear staining decreases in parallel to transcriptional silencing in spermatogenesis (Figure 5A), and xSAHH was not detected by two-dimensional polypeptide analysis of differentiated erythrocytes (protein 21; Dreyer and Hausen, 1983). In the female germ line, higher amounts of nuclear xSAHH are found in oogonia than during the subsequent stages of the meiotic prophase. Increasing amounts were detected in the growing diplotene oocytes that synthesize the pool of maternal mRNA

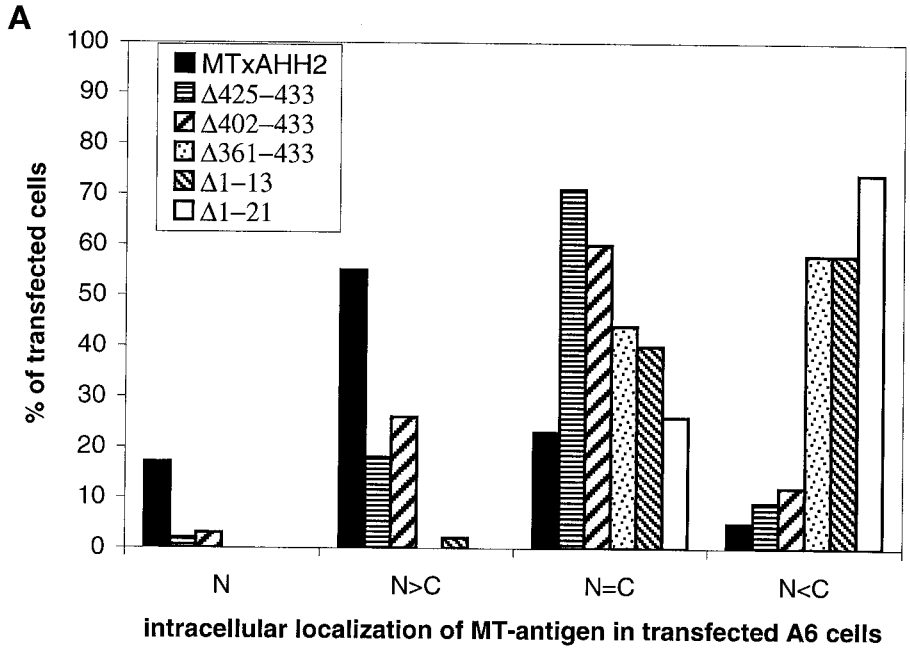

B

N-terminus

wtMT-xAHH2	1	*MEQKLISEEDL*NSARGEISLLFT **MSDKLSYKVA DISLADWGRK AIEIAENEMP GLMKMREMYS ESKPLKGARIA** 50
xAHHΔ1-13	14	*MEQKLISEEDL*NSARGEIPSSSP CLTNCPTKSL TSG**LADWGRK AIEIAENEMP GLMKMREMYS ESKPLKGARIA** 50
xAHHΔ1-21	22	*MEQKLISEEDL*NSARGEIPSSSP CLTNCPTKSL TSAWPTGAGR P**IEIAENEMP GLMKMREMYS ESKPLKGARIA** 50

C-terminus

wt-xAHH2	360	**PSFVMS NSFTNQVMAQ IELWTNTDKY PVGVYFLPKK LDEAVAAAHL DKLGVKLTKL TDKQAKYLGL DKEGPFKPDH YRY*** 433
xAHHΔ425-433	360	**PSFVMS NSFTNQVMAQ IELWTNTDKY PVGVYFLPKK LDEAVAAAHL DKLGVKLTKL TDKQAKYLGL DKEG**LEPLE L* 424
xAHHΔ402-433	360	**PSFVMS NSFTNQVMAQ IELWTNTDKY PVGVYFLPKK LDEAVAAAHL D**QTGSQAHQADRQTSQVSWAG* 401
xAHHΔ361-433	360	**PSFVMS**SL*

Figure 8. Influence of N-terminal and C-terminal deletions on intracellular localization of MT-xSAHH in transfected A6 cells. (A) Full-length MT-xSAHH or the truncated forms explained in B were expressed in A6 cells after transient transfection. The percentages of transfected cells showing localization of the MT-xSAHH exclusively (N) or predominantly in the nucleus (N>C), in the cytoplasm (C>N), or at similar levels in both compartments (N=C) are compiled from two or three independent experiments and plotted. Several hundred cells were analyzed for each individual fusion protein, except for xSAHHΔ361–433, where n was 165, because this product was either toxic or unstable, resulting in a low percentage of evaluable cells. (B) The N terminus and the C terminus of the fusion proteins encoded by the cDNAs used for transfection are shown, with numbers referring to the wt-xSAHH2 aa sequence. Only the last of six N-terminal myc tags are shown in italics. The original xSAHH sequence is shown in bold letters; linker sequence is shown in plain uppercase letters; and aa exchanged by mutagenesis are underlined.

(Wedlich and Dreyer, 1988). Furthermore, there is a functional link between SAHH activity and hnRNA synthesis, because inhibitors of SAHH interfere with methylation of poly(A)$^+$ RNA and with its synthesis, probably because of an arrest of elongation if cap methylation does not occur (Figure 6). Our present evidence primarily supports a role of xSAHH in RNA methylation. In addition, nuclear proteins could be targets of SAM-dependent methylation processes. Among the potential targets associated with RNA export from the nucleus are heterogeneous nuclear ribonucleoproteins known to be methylated on arginine residues (Shen *et al.*, 1998).

Structural Requirements for Nuclear Translocation of xSAHH in Transfected Cells

Because the conserved primary amino acid sequence of SAHH lacks a bona fide nuclear localization signal, we have initiated a mutational analysis to identify the parts of the molecule that are required for its nuclear accumulation. The molecular size of the xSAHH monomer would, in principle, permit translocation through the nuclear pores by diffusion, although at a very low rate. The observation that deletion of either C-terminal or N-terminal parts of the enzyme impedes or even precludes its accumulation in the nucleus argues against passive diffusion and suggests a mechanism involving sequence-specific protein interaction. Furthermore, the observation that nuclear translocation appeared to be retarded in cells expressing particularly high amounts of the xSAHH proteins suggests a saturable transport or anchoring mechanism.

Whereas the wild-type xSAHH was predominantly nuclear in transfected A6 cells, substitution of the 13 N-terminal aa of xSAHH highly reduced and substitution of the 21 N-terminal aa virtually prevented the accumulation of the fusion protein in the nuclei. Both N-terminal mutations affect a putative α-helical domain in xSAHH. The recently published crystal structure of the rat SAHH reveals an α-helix between aa 13 and 25 (Hu *et al.*, 1999), predicted to be at the surface of the tetrameric enzyme. This region is therefore a likely candidate for protein–protein interactions. Interestingly, replacement of nine C-terminal amino acids, including K^{427}, which has previously been shown to be essential for tetramer formation and for enzyme activity of the human SAHH (Ault-Riche *et al.*, 1994), significantly reduced, but did not preclude, nuclear localization of xSAHH. A longer C-terminal truncation, Δ361–433, totally prevented nuclear accumulation of xSAHH. These observations indicate that nuclear translocation of xSAHH may require more than a single linear signal. Interacting surfaces of both the N terminus and the C terminus of xSAHH may contribute to its nuclear accumulation.

Conditional nuclear accumulation of the enzyme xSAHH could depend on regulated nuclear translocation mediated by cell type or cell cycle–specific carriers belonging to the importin–karyopherin family or by masking and unmasking of nuclear translocation signals and nuclear export signals. This could depend on conformational changes of the enzyme itself or on the presence of binding partners. Alternatively, xSAHH could be able to shuttle between the nucleus and the cytoplasm, and its predominant localization would be directed by the abundance of binding partners in each compartment. The distinction between different mechanisms of nuclear retention may be possible after the identification of the hypothetical binding partners.

ACKNOWLEDGMENTS

We thank Claudia Mohl for protein purification and isolation of cDNAs in the course of her diploma thesis (University of Tuebingen, 1996). We are greatly indebted to Prof. Klaus Weber and Uwe Plessmann for peptide microsequencing. We thank Drs. Francois Fagotto, Reimer Stick, and Neil Armstrong for many helpful comments on the manuscript, Brigitte Gläser for technical advice, Ulrike Goßweiler for tissue culture work and figure layout, and Hülya Wicher for secretarial help.

REFERENCES

Araujo, F.D., Knox, J.D., Szyf, M., Price, G.B., and Zannis-Hadjopoulos, M. (1998). Concurrent replication and methylation at mammalian origins of replication. Mol. Cell. Biol. *18*, 3475–3482.

Ault-Riche, D.B., Yuan, C.S., and Borchardt, R.T. (1994). A single mutation at lysine 426 of human placental *S*-adenosylhomocysteine hydrolase inactivates the enzyme. J. Biol. Chem. *269*, 31472–31478.

Bachvarova, R., and Davidson, E.H. (1966). Nuclear activation at the onset of amphibian gastrulation. J. Exp. Zool. *163*, 285–296.

Bergmann, S., Shatrov, V., Ratter, F., Schiemann, S., Schulze-Osthoff, K., and Lehmann, V. (1994). Adenosine and homocysteine together enhance TNF-mediated cytotoxicity but do not alter activation of nuclear factor-kappa B in L929 cells. J. Immunol. *153*, 1736–1743.

Bestor, T.H. (1992). Activation of mammalian DNA methyltransferase by cleavage of a Zn binding regulatory domain. EMBO J. *11*, 2611–2617.

Bird, A., Taggart, M., and Macleod, D. (1981a). Loss of rDNA methylation accompanies the onset of ribosomal gene activity in early development of *X. laevis*. Cell *26*, 381–390.

Bird, A.P. (1986). CpG-rich islands and the function of DNA methylation. Nature *321*, 209–213.

Bird, A.P., Taggart, M.H., and Gehring, C.A. (1981b). Methylated and unmethylated rRNA genes in the mouse. J. Mol. Biol. *152*, 1–17.

Bregman, D.B., Du, L., van der Zee, S., and Warren, S.L. (1995). Transcription-dependent redistribution of the large subunit of RNA polymerase II to discrete nuclear domains. J. Cell. Biol. *129*, 287–298.

Breschi, L., Mazzotti, G., Baratta, B., Galanzi, A., Strocchi, P., Falconi, M., Centurione, M.A., Ferrari, C., and Rizzoli, R. (1998). Immunocytochemical discrimination between early and late S phase: a new approach to the study of gingival epithelium proliferation in rats. J. Periodontol. *69*, 84–91.

Cooper, D.N., Taggart, M.H., and Bird, A.P. (1983). Unmethylated domains in vertebrate DNA. Nucleic Acids Res. *11*, 647–658.

Crease, D.J., Dyson, S., and Gurdon, J.B. (1998). Cooperation between the activin and Wnt pathways in the spatial control of organizer gene expression. Proc. Natl. Acad. Sci. USA *95*, 4398–4403.

Dreyer, C. (1987). Differential accumulation of oocyte nuclear proteins by embryonic nuclei of *Xenopus*. Development *101*, 829–846.

Dreyer, C. (1989). Fate and nuclear localization of germinal vesicle proteins during embryogenesis. In: Genomic Adaptability in Cell Specialization of Eukaryotes. Embryology, a Comprehensive Synthesis, vol. 6, ed. M.A. Di Berardino and L. Etkin, New York: Plenum Press, 31–57.

Dreyer, C., and Hausen, P. (1983). Two-dimensional gel analysis of the fate of oocyte nuclear proteins in the development of *Xenopus laevis*. Dev. Biol. *100*, 412–425.

Dreyer, C., Scholz, E., and Hausen, P. (1982). The fate of oocyte nuclear proteins during early development in *Xenopus laevis*. Wilhelm Roux's Arch. Dev. Biol. *191*, 228–233.

Dreyer, C., Singer, H., and Hausen, P. (1981). Tissue specific nuclear antigens in the germinal vesicle of *Xenopus laevis* oocytes. Wilhelm Roux's Arch. Dev. Biol. *190*, 197–207.

Dreyer, C., Wang, Y.H., and Hausen, P. (1985). Immunological relationship between oocyte nuclear proteins of *Xenopus laevis* and *X. borealis*. Dev. Biol. *108*, 210–219.

Ellinger-Ziegelbauer, H., and Dreyer, C. (1993). The pattern of retinoic acid receptor gamma (RAR gamma) expression in normal development of *Xenopus laevis* and after manipulation of the main body axis. Mech. Dev. *41*, 33–46.

Fabianowska-Majewska, K., Duley, J.A., and Simmonds, H.A. (1994). Effects of novel antiviral adenosine analogues on the activity of *S*-adenosylhomocysteine hydrolase from human liver. Biochem. Pharmacol. *48*, 897–903.

Fagotto, F., and Gumbiner, B.M. (1994). Beta-catenin localization during *Xenopus* embryogenesis: accumulation at tissue and somite boundaries. Development *120*, 3667–3679.

Gall, J.G. (1998). Spread preparations of *Xenopus* germinal vesicle contents. In: Cell Biology: A Laboratory Manual, ed. D. Spector, R. Goldman, and L. Leinwand, Cold Spring Harbor, NY: Cold Spring Harbor Laboratory Press, 3.1–3.3.

Gall, J.G., and Murphy, C. (1998). Assembly of lampbrush chromosomes from sperm chromatin. Mol. Biol. Cell *9*, 733–747.

Gruenbaum, Y., Stein, R., Cedar, H., and Razin, A. (1981). Methylation of CpG sequences in eukaryotic DNA. FEBS Lett. *124*, 67–71.

Hausen, P., Wang, Y.H., Dreyer, C., and Stick, R. (1985). Distribution of nuclear proteins during maturation of the *Xenopus* oocyte. J. Embryol. Exp. Morphol. *89*, 17–34.

Heby, O. (1995). DNA methylation and polyamines in embryonic development and cancer. Int. J. Dev. Biol. *39*, 737–757.

Heldin, C.H., Miyazono, K., and ten Dijke, P. (1997). TGF-beta signaling from cell membrane to nucleus through SMAD proteins. Nature *390*, 465–471.

Hershfield, M.S., and Krodich, N.M. (1978). *S*-Adenosylhomocysteine hydrolase is an adenosine-binding protein: a target for adenosine toxicity. Science *202*, 757–760.

Hu, Y.B., Komoto, J., Huang, Y., Gomi, T., Ogawa, H., Takata, Y., Fujioka, M., and Takusagawa, F. (1999). Crystal structure of *S*-adenosylhomocysteine hydrolase from rat liver. Biochemistry *38*, 8323–8333.

Jackson, D.A., Hassan, A.B., Errington, R.J., and Cook, P.R. (1993). Visualization of focal sites of transcription within human nuclei. EMBO J. *12*, 1059–1065.

Kirillov, A., Kistler, B., Mostoslavsky, R., Cedar, H., Wirth, T., and Bergman, Y. (1996). A role for nuclear NF-kappaB in B-cell-specific demethylation of the Igkappa locus. Nat. Genet. *13*, 435–441.

Kramer, D.L., Porter, C.W., Borchardt, R.T., and Sufrin, J.R. (1990). Combined modulation of *S*-adenosylmethionine biosynthesis and *S*-adenosylhomocysteine metabolism enhances inhibition of nucleic acid methylation and L1210 cell growth. Cancer Res. *50*, 3838–3842.

Liu, F., Pouponnot, C., and Massague, J. (1997). Dual role of the Smad4/DPC4 tumor suppressor in TGFbeta-inducible transcriptional complexes. Genes & Dev. *11*, 3157–3167.

Matsuo, K., Silke, J., Georgiev, O., Marti, P., Giovannini, N., and Rungger, D. (1998). An embryonic demethylation mechanism involving binding of transcription factors to replicating DNA. EMBO J. *17*, 1446–1453.

Mazzotti, G., Gobbi, P., Manzoli, L., and Falconi, M. (1998). Nuclear morphology during the S phase. Microsc. Res. Tech. *40*, 418–431.

McCracken, S., Fong, N., Rosonina, E., Yankulov, K., Brothers, G., Siderovski, D., Hessel, A., Foster, S., Shuman, S., and Bentley, D.L. (1997). 5′-Capping enzymes are targeted to premRNA by binding to the phosphorylated carboxy-terminal domain of RNA polymerase II. Genes & Dev. *11*, 3306–3318.

Messmer, B., and Dreyer, C. (1993). Requirements for nuclear translocation and nucleolar accumulation of nucleolin of *Xenopus laevis*. Eur. J. Cell Biol. *61*, 369–382.

Miller, M., Reddy, B.A., Kloc, M., Li, X.X., Dreyer, C., and Etkin, L.D. (1991). The nuclear-cytoplasmic distribution of the *Xenopus* nuclear factor, xnf7, coincides with its state of phosphorylation during early development. Development *113*, 569–575.

Miller, M.W., Duhl, D.M., Winkes, B.M., Arredondo-Vega, F., Saxon, P.J., Wolff, G.L., Epstein, C.J., Hershfield, M.S., and Barsh, G.S. (1994). The mouse lethal nonagouti (a(x)) mutation deletes the *S*-adenosylhomocysteine hydrolase (Ahcy) gene. EMBO J. *13*, 1806–1816.

Monk, M., Boubelik, M., and Lehnert, S. (1987). Temporal and regional changes in DNA methylation in the embryonic, extraembryonic and germ cell lineages during mouse embryo development. Development *99*, 371–382.

Newport, J., and Kirschner, M. (1982a). A major developmental transition in early *Xenopus* embryos: I. characterization and timing of cellular changes at the midblastula stage. Cell *30*, 675–686.

Newport, J., and Kirschner, M. (1982b). A major developmental transition in early *Xenopus* embryos: II. Control of the onset of transcription. Cell *30*, 687–696.

Niewkoop, P., and Faber, J. (1967). Normal table of *Xenopus laevis* (Daudin). Amsterdam: North Holland Publishing.

Nomura, M., and Li, E. (1998). Smad2 role in mesoderm formation, left-right patterning and craniofacial development. Nature *393*, 786–790.

Pudney, M., Varma, M.G., and Leake, C.J. (1973). Establishment of a cell line (XTC-2) from the South African clawed toad, *Xenopus laevis*. Experientia *29*, 466–467.

Rizzoli, R., Baratta, B., Maraldi, N.M., Falconi, M., Galanzi, A., Papa, S., Vitale, M., Rizzi, E., Manzoli, L., and Mazzotti, G. (1992). DNA synthesis progression in 3T3 synchronized fibroblasts: a high resolution approach. Histochemistry *97*, 181–187.

Rupp, R.A., Snider, L., and Weintraub, H. (1994). *Xenopus* embryos regulate the nuclear localization of XMyoD. Genes & Dev *8*, 1311–1323.

Sambrook, J., Fritsch, E.F., and Maniatis, T. (1989). Molecular Cloning: A laboratory manual. Cold Spring Harbor, NY: Cold Spring Harbor Laboratory Press.

Schneider, S., Steinbeisser, H., Warga, R.M., and Hausen, P. (1996). Beta-catenin translocation into nuclei demarcates the dorsalizing centers in frog and fish embryos. Mech. Dev. *57*, 191–198.

Schwab, M.S., and Dreyer, C. (1997). Protein phosphorylation sites regulate the function of the bipartite NLS of nucleolin. Eur. J. Cell Biol. *73*, 287–297.

Seery, L.T., McCabe, B.D., Schoenberg, D.R., and Whitehead, A.S. (1994). *S*-Adenosyl-L-homocysteine hydrolase from *Xenopus laevis*—identification, developmental expression and evolution. Biochem. Biophys. Res. Commun. *205*, 1539–1546.

Shen, E.C., Henry, M.F., Weiss, V.H., Valentini, S.R., Silver, P.A., and Lee, M.S. (1998). Arginine methylation facilitates the nuclear export of hnRNP proteins. Genes & Dev. *12*, 679–691.

Suzuki, A., Chang, C., Yingling, J.M., Wang, X.F., and Hemmati-Brivanlou, A. (1997). Smad5 induces ventral fates in *Xenopus* embryo. Dev. Biol. *184*, 402–405.

Turner, D.L., and Weintraub, H. (1994). Expression of achaete-scute homolog 3 in *Xenopus* embryos converts ectodermal cells to a neural fate. Genes & Dev. *8*, 1434–1447.

Turner, M.A., Dole, K., Yuan, C., Hershfield, M.S., Borchardt, R.T., and Howell, L.P. (1997). Crystallization and preliminary x-ray analysis of human placental *S*-adenosylhomocysteine hydrolase. Acta Crystallogr. *D53*, 339–341.

Ueland, P.M. (1982). Pharmacological and biochemical aspects of *S*-adenosylhomocysteine and *S*-adenosylhomocysteine hydrolase. Pharmacol. Rev. *34*, 223–253.

Wansink, D.G., Schul, W., van der Kraan, I., van Steensel, B., van Driel, R., and de Jong, L. (1993). Fluorescent labeling of nascent RNA reveals transcription by RNA polymerase II in domains scattered throughout the nucleus. J. Cell Biol. *122*, 283–293.

Wedlich, D., and Dreyer, C. (1988). Cell specificity of nuclear protein antigens in the development of *Xenopus* species. Cell Tissue Res. *252*, 479–489.